LES evaluation of wind pressures on a standard tall building with and without a neighboring building

Agerneh K. Dagnew[a], Girma T. Bitsuamlak[b]
[a]*PhD candidate, Civil and Environmental Eng. (CEE) Dept./ International Hurricane Research Center (IHRC), Florida International University (FIU), Miami, Florida, adagn001@fiu.edu*
[b]*Assistant Professor, CEE / IHRC, FIU, Miami, Florida, bitsuamg@fiu.edu*

ABSTRACT: External turbulent wind induced aerodynamic loads are computationally evaluated for a standard tall building known as Commonwealth Advisory Aeronautical Research Council (CAARC) model (Melbourne, 1980) also used by several wind engineering laboratories for calibration purposes. In addition to evaluating wind pressures on isolated CAARC model building, the present study investigated sheltering effects due to an adjacent building placed in close proximity. Large eddy simulation (LES), a multi-scale computational modeling approach that offers a more comprehensive way of capturing fluctuating turbulent flow, have been employed in all simulations. Numerically obtained wind induced pressure coefficients on the façade of CAARC model building under different configurations have been compared with boundary layer wind tunnel data (BLWT). For cross comparison purposes, numerically obtained external pressure coefficients from literature have been compared with the current numerical results. An acceptable agreement between the numerical and wind tunnel mean pressure coefficients has been observed.

KEY WORDS: Computational fluid dynamics (CFD), boundary layer wind tunnel, wind pressure, tall building, LES, power spectrum, pressure coefficients.

1 INTRODUCTION

Several studies on flow past an isolated square or rectangular building have been carried researchers in wind engineering area by using mostly wind tunnel and more recently by a numerical approach. Recent advances in hardware and software technology coupled with development of reliable sub-grid turbulence models and numerical generation of inflow turbulence, which account effects of upstream terrain makes, numerical wind load evaluation an attractive proposition (Tamura et al., 2008). The majority of numerical prediction of wind pressure loads on buildings have been devoted on the basic cube shape immersed in turbulent boundary layer flow, because of its geometrical simplicity yet representing the basic complex features of building aerodynamics and availability of experimental data (Lim et al., 2009; Stathopoulos and Wu, 2004). The focuses of the numerical evaluation have been on both short and tall buildings. Commonly studied full-scale low-rise buildings include Silsoe Cube (Wright and Easom, 2003), Texas Tech (Senthooran et al. 2004) and Wall of Wind test building (Bitsuamlak et al. 2010). Some of the studies carried out on high-rise building include (Nozawa and Tamura, 2002; Tominaga et al. 2008a), and others. Huang et al (2007) and Braun and Awruch (2009) studied the external aerodynamics of CAARC building and investigated flow patterns, mean and root-mean-square (rms) pressure coefficients on the building perimeter.

With other buildings present in close proximity, the dynamics of the flow become much more complex and flow interference occurs (Khandure et al. 1998). The most commonly reported in-

terference effects are (a) sheltering which leads to reduction of drag force on the downstream building and amplification of the fluctuating force due to turbulence buffeting (Thepmongkorn et al. 2002;Lam et al. 2008), (b) flow channeling due to close spacing of buildings (Princevac et al. in press), (c) flow asymmetry which could possibly introduce wind –induced torsion, and (d) wake buffeting. Most of the preexisting numerical studies for assessment and evaluation of interference effects employed the most commonly used Reynolds-averaged Navier-Stokes (RANS) equations (Lam et al. 2008; Zhang and Gu, 2008; Lam and To, 2006). The numerical simulation of the present study involves assessment of effects of inflow turbulence with the use large eddy simulation (LES) and validation with wind tunnel data obtained from RWDI USA LLC, Miramar FL (Dagnew et al. 2009).

2 GENERAL OUTLINE OF WIND TUNNEL TESTING

The wind tunnel testing facility has a testing section of 8.5ft wide by 7ft tall. The floor has mechanical systems which monitor the degree of surface roughness. Approximately 1in by 1 in flat plate on 12 in x12in diamond pattern roughness cubes are used to replicate open terrain type surface roughness. The CAARC model building has a rectangular prismatic shape with dimensions 100 ft (x) by 150 ft (y) by 600 ft (z) height. The experiment has been done using a 1:400 scale rigid (aerodynamic) model under different configuration as shown in Fig. 1. The Reynolds number based on building height H and inflow velocity U_H = 12.12 m/s, measured at 4ft upwind of test building, is $3x10^5$. Open exposure with "power low exponent of 0.16" is assumed.

Table 1 CFD simulation cases

Case	Configuration	Wind angle of attack	y_+
Case 1	isolated	0^0	$1 < y_+ < 5$
Case 2	full height adj. bldg downwind of CAARC	0^0	$1 < y_+ < 5$
Case 3	full height adj. bldg upwind of CAARC	0^0	$30 < y_+ < 300$
Case 4	half height adj. bldg upwind of CAARC	0^0	$30 < y_+ < 300$
Case 5	full height adj. bldg to the side of CAARC	0^0	$30 < y_+ < 300$

3 OUTLINE OF CFD MODELING

3.1 *Geometrical layout and study cases*

The geometrical modeling adopted for the CFD simulation of CAARC building, mimics the 1:400 scale wind tunnel aerodynamic model. The wind flow is described in a Cartesian coordinate system (x, y, z), in which the x-axis is aligned with the stream-wise direction, the z-axis is in the lateral direction and the y-axis is in the vertical direction. In the present study, three building configurations have been investigated. Table 1 describes all CFD simulation cases considered.

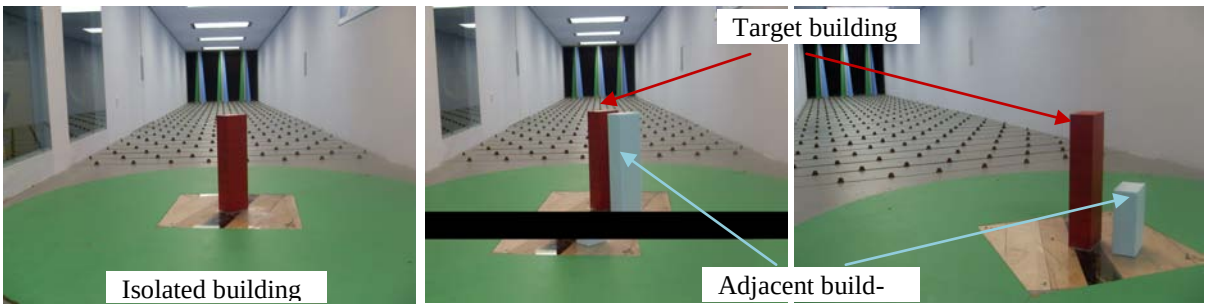

Figure 1 Wind tunnel testing configuration

3.2 *Computational domain (CD)*

CD defines the region where the flow field is computed. The size of the CD should be large enough to accommodate all relevant features that will have potential effects in altering the character of the flow field in the region of interest. In most cases, the stretch of the CD in the vertical, lateral and flow direction depends on the type of boundary conditions. Franke et al (2006) and COST (2007) suggested that for a single building of height H, vertically the domain should extend 4H to 5H above the roof level if smaller blockage and up to 10H if larger blockage is anticipated. Based on these recommendations and from author's previous experience, the CD extends 5H upwind and 15H downstream of the target building. Laterally it extends 5H from the side wall surfaces and top boundary is placed at 3H above the roof of the target building (Fig. 2b).

3.3 *Boundary conditions*

Boundary conditions represent the surroundings that have been cut off by the CD and idealize the influence of the actual flow environment under consideration. It determines the solution inside the assumed CD and has significant effects on the accuracy of the prediction. At the inlet boundary, the mean velocity profile obeys power law profile as the wind tunnel testing (Fig. 2a). Unlike steady RANS simulations, for LES time dependent inflow boundary is responsible for accurate representation of oncoming flow properties. Numerically simulated oncoming turbulent flow should possess the inherent characteristic of natural wind (Tamura et al. 2008). There are various techniques to generate inflow turbulence computationally. Kondo et al (1997) for example used Monte Carlo simulation technique for reproduction of inflow turbulences. Others use an auxiliary CD to estimate the boundary parameters from the computed result of the driver section (Lund, 1998). Nozawa and Tamura (2002) subsequently extend Lund's method and employed it to rough-wall boundary-layer flow. Fluent Inc. (2006) uses random flow generation technique and compute fluctuating velocity components by using synthesizing a divergence-free velocity-vector field from the summation of Fourier harmonics. Figure 3a and b describe stream-wise and power spectrum of lateral velocity fluctuations, respectively, at a control point measured behind CAARC model. While LES with inflow turbulence produced more velocity fluctuation downstream of test building, LES without inflow perturbation relatively dampened the fluctuation (Fig 3a). Figure 3b shows the power spectrum of LES with inflow perturbation case.

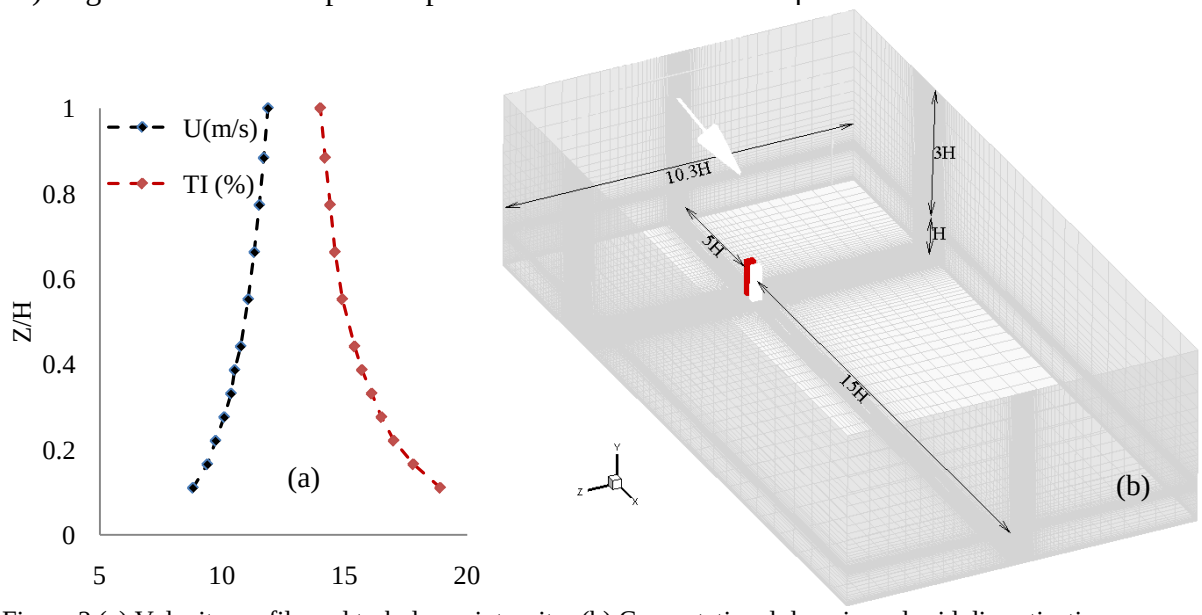

Figure 2 (a) Velocity profile and turbulence intensity; (b) Computational domain and grid discretization.

Near solid wall surface, in which viscosity of the fluid dominates the flow, the direct viscosity effect is usually neglected in deriving the main turbulence equations (Franke et al. 2006). Numerically simulated mean velocity profile and turbulence quantities are representative of the actual terrain characteristics that are not included in the CD. To address the roughness, the shear stress can be evaluated from the logarithmic relationship incorporated in the momentum equation between the wall and the first grid point (Mochida et al. 2002; Bitsuamlak et al. 2005). Blocken et al (2007), who reviewed works of various researchers emphasized on the effect of surface roughness in generating homogeneous mean velocity profile and turbulent kinetic energy. Although researchers have commented on the inadequacy of a smooth wall assumption, because of its relative ease several studies have been done without considering effect of surface roughness (Tominaga et al. 2008a; Yoshie et al. 2007). Murakami (1998) discussed the ineffectiveness of the no-slip boundary when applied to a bluff body with high Reynolds (Re) number and advised use of Werner and Wengle (1991) wall function. Hence this boundary is applied at the wall surfaces. Symmetry boundary condition is employed at the top and lateral surfaces. Since details of the flow variables are not known prior to the simulation, an outflow boundary was applied at the outlet plane.

3.4 *Grid discretization*

For turbulent flow, COST (2007) and Tominaga et al (2008b) suggested that the grid stretching ratio should be less than 1.3. However, it is customary to conduct grid sensitivity analysis and confirm that the results would no longer be affected by changing the grid arrangement (Blocken et al. 2007; Yoshie et al. 2007). In LES simulation use of excessive stretching ratio usually causes numerical divergence due to the fact that the cut-off wave number of the energy spectrum between resolved and subgrid-scale is related to grid size. Therefore, use of smaller stretching ratio (1.05) is advised as it would possible suppressed numerical oscillation (Murakami, 1998). Two cases of hexahedral grids were generated, for Case 1 and Case 2 high resolution boundary layer mesh with $y_p = 10^{-5}$ and stretching ratio of 1.05 was generated (Table 1). For other cases coarser mesh with $y_p = 0.001$ was used and non dimensional wall unit was maintained between $30 < y+ < 300$.

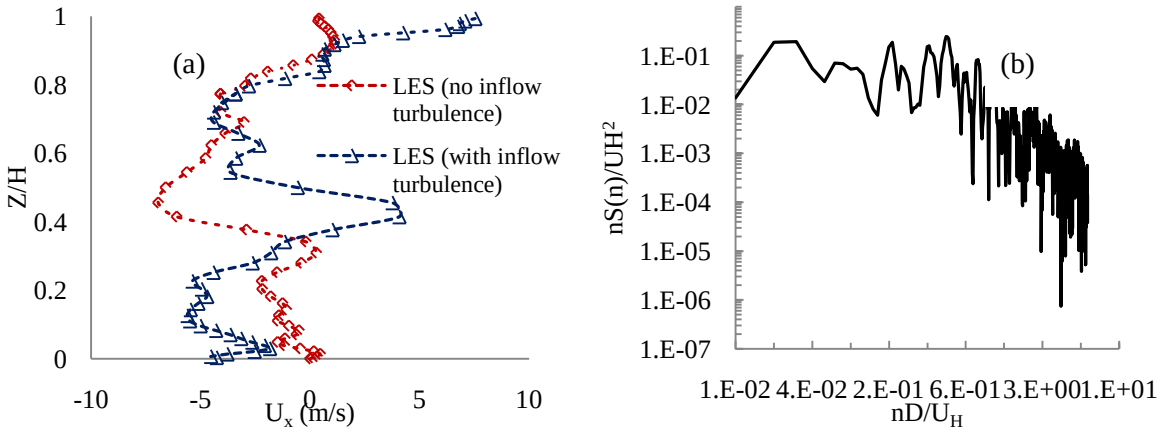

Figure 3 (a) Stream-wise velocity distribution downwind of CAARC model; (b) power spectrum of lateral velocity.

3.5 *Turbulence modeling and Numerical Scheme*

RANS and LES are the two most widely used models for evaluation of wind effects on structures. RANS mainly relies on statistical approaches that give a time-mean representation of the flow in question. In contrast, LES is a multi-scale computational modeling approach that offers a more comprehensive way of capturing fluctuating turbulent flow. Dynamic Smagornisky-Lilly model have been only used for Case 5 and dynamic SGS kinetic energy models were used for all other cases.

4 RESULT AND DISCUSSION

As a control case, preliminary exploratory study on isolated CAARC model building (Case 1) has been carried out. Two types of mesh were generated, as explained in section 3.4, and mean and r.m.s pressure coefficients measured at 2/3H of the building height have been compared with BLWT data. Figure 6a shows comparison between numerically obtained pressure coefficients on perimeter of isolated CAARC model building with the BLWT data. While for one case (LES1), high resolution meshes were used in the near-wall region to resolve the low Reynolds number flow up to the wall surface and Werner and Wengle (1991) wall functions are applied for another case (LES2). The comparison revealed that LES1 shows better agreement with BLWT data and previous CFD data from literature (Huang et al. 2007; Braun and Awruch, 2009). The near-wall treatment has contributes to the prediction accuracy of the numerical simulation as observed from result of LES2. Around the sharp corner where flow separation occurs, LES2 deviates from the wind tunnel measurements and noticeable discrepancies have been observed.

The r.m.s. pressure coefficient obtained using Paterson's (1993) methods is comparable with the BLWT and previous CFD results (Huang et al. 2007; Braun and Awruch, 2009) as shown in Fig. 6c. Presence of a neighboring building alters the aerodynamic characteristics. The present study attempted to assess these changes numerically. Cases 2 and 3 represent CAARC model with a full height neighboring building, Case 4 with half height in tandem arrangement and Case 5 with full height placed side by side with the model building (Table 1). Space separation, based on larger width (B) of the building was kept at S/B = 0.67. Figure 6b shows the sheltering effect of neighboring buildings. From the CFD prediction it has been observed that Case 2 showed almost 25% increase in mean wind pressures coefficients on windward face compared to Case 1 (Fig. 4b). There is also considerable increase in negative pressure loads on the side faces. Case 3 illustrated a typical sheltering effect by an upwind building and experienced negative pressure on the windward face.

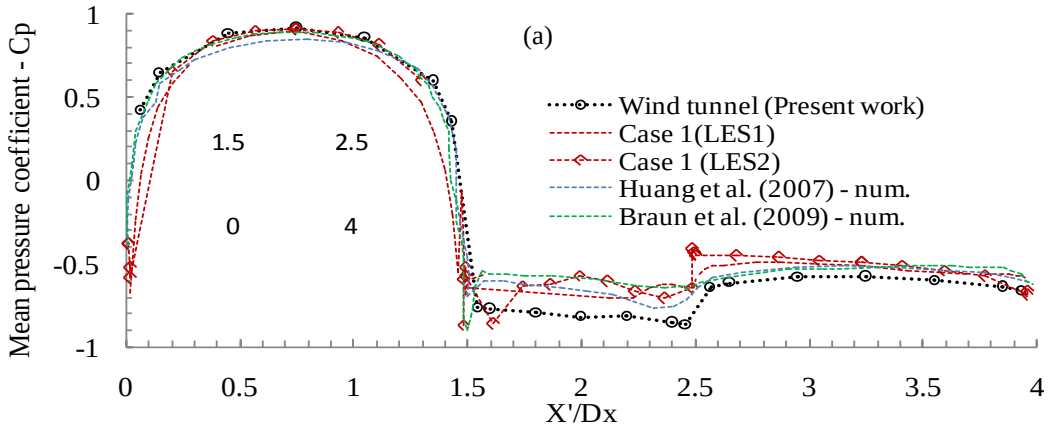

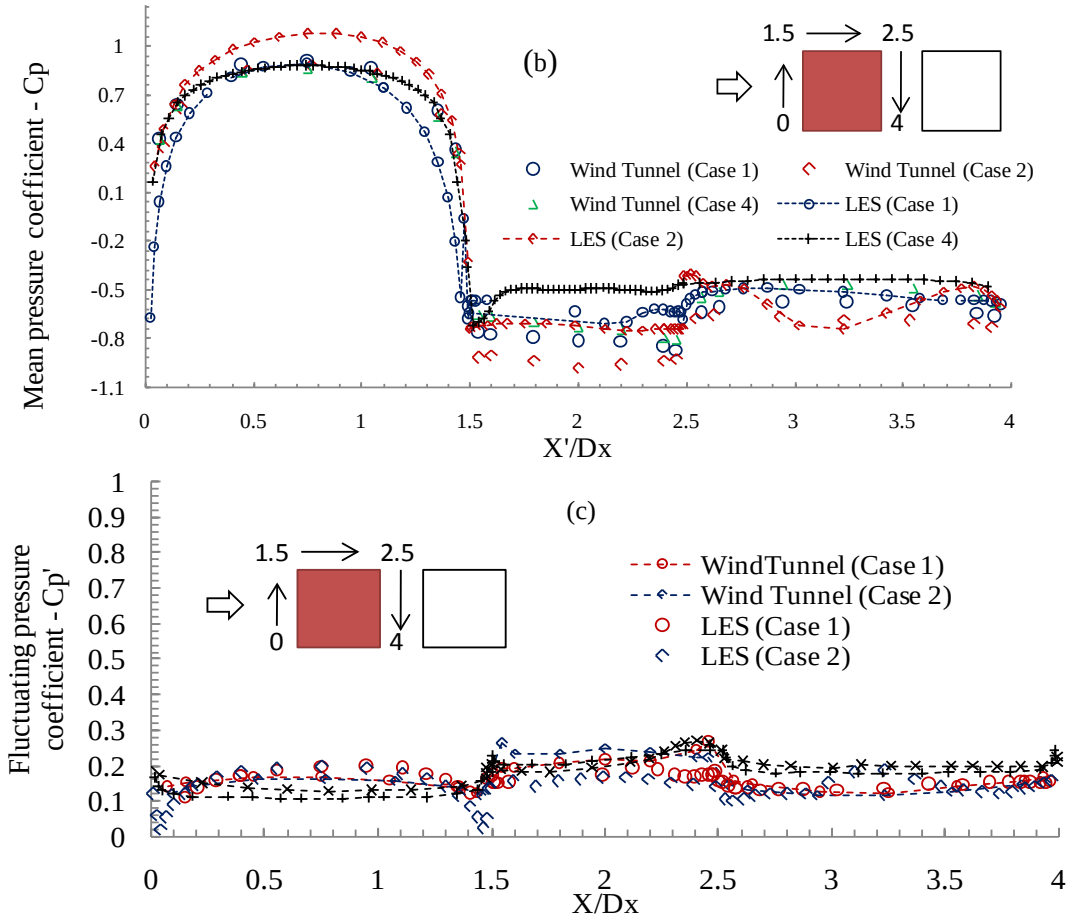

Figure 4 Comparison and validation of mean and r.m.s. pressure coefficients over the building perimeter at Z/H = 2/3: (a) Case 1; (b) Case 1, 2 and 4; (c) Case 1&2

4.1 *Flow field visualization*

Figure 5a presents representative mean-pressure contour plots for windward faces of Case 1 and 4 configurations. For Case 1, the horseshoe vortex shape contour generated on the front wall agrees well with studies by Huang et al (2007) and Braun and Awruch (2009). While Cases 2 and 4 showed smaller and modified horseshoe vortex on windward faces. For Case 5 asymmetry pressure coefficient distributions on the front walls and more negative pressures on the side walls have been observed due to channeling effects. Fluctuating components and alternative vortex shedding are numerically reproduced with LES turbulence modeling as shown in velocity contour filed of Figure 5b.

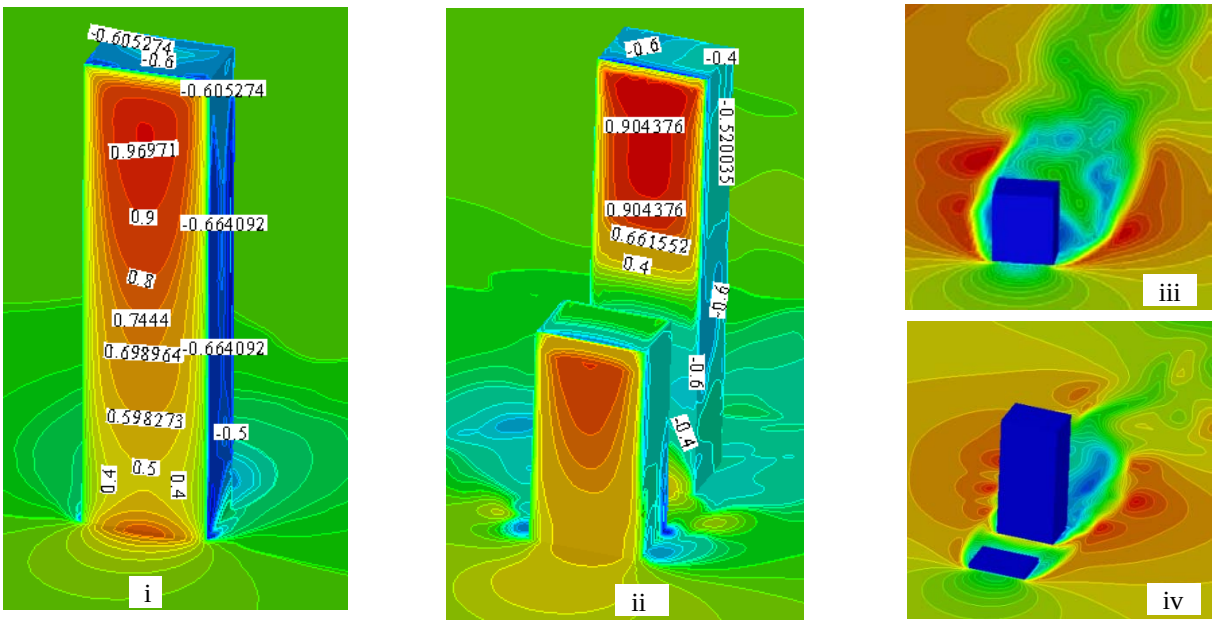

Figure 5 (a) Typical mean pressure coefficient: (i) Case 1, (ii) Case 4; (b) typical velocity magnitude contours of CAARC and neighboring building surfaces respectively at 2/3H: (iii) Case I; (iv) Case 4

5 CONCLUSIONS

Computational assessment of aerodynamic characteristics of a typical tall building (CAARC) with and without neighboring building were performed and results were compared with BLWT data. LES with inflow turbulence perform better and captured velocity fluctuations. Sheltering effects have been captured by the numerical simulation when adjacent buildings are placed upwind of the study building. Mean pressure coefficient increased for Case 2 when compared with isolated CAARC model (Case 1). Flow channeling resulted in asymmetric pressure distribution when adjacent buildings were placed side-by-side to the CAARC model. Work in progress includes generating the time history of the pressure at different locations, drag and lifts force coefficients and comparison of wake power spectrum for all cases.

6 ACKNOWLGMENT

This material is based in part upon work supported by the National Science Foundation CAREER project under Grant Number 0846811. Any opinions, findings, and conclusions or recommendations expressed in this material are those of the author(s) and do not necessarily reflect the views of the National Science Foundation. This research was supported in part by the National Science Foundation through TeraGrid resources provided by National Center for Supercomputing Applications (NCSA). We are grateful to RWDI Miramar Inc. for providing us with the wind tunnel data used for comparison purposes.

7 REFERENCES

Bitsuamlak, G.T., Stathopoulos, T., Bédard, C. 2005. Effect of upstream hills on design wind load: a computational approach . Wind and Structures. Vol. 9, No. 1, 37-58 .

Bitsuamlak, G.T., Dagnew, A.K., and Chowdhury, A.G. 2010. Computational assessment of blockage and wind simulator proximity effects for a new full-scale testing facility 13. Wind and Structures. Vol. 13 No. 1, 21-36.

Blocken, B., Stathopoulos, T., Carmeliet, J. 2007. CFD simulation of the atmospheric boundary layer: wall function problems. Atmospheric Environment 41, 238-252.

Braun, A.L., Awruch, A.M. 2009. Aerodynamic and aeroelastic analyses on the CAARC standard tall building model using numerical simulation. Computers and Structures 87, 567-581.

COST. 2007. Best practice guideline for the CFD simulation of flows in the urban environment COST Action 732.

Dagnew, A.K., Bitsuamalk, G.T., Ryan, M. 2009. Computational evaluation of wind pressures on tall buildings. 11th American conference on Wind Engineering. San Juan, Puerto Rico

Fluent Inc. 2006. Fluent 6.3 User's Guide. Fluent Inc., Lebanon. 6.3.26.

Franke. J. 2006. Recommendations of the COST action C14 on the use of CFD in predicting pedestrian wind environment. The Fourth International Symposium on Computational Wind Engineering.

Huang, S., Li, Q.S., Xu, S. 2007. Numerical evaluation of wind effects on a tall steel building by CFD. Journal of Constructional Steel Research 63, 612-627.

Khandure, A.C., Stathopoulos, T., Bedard, C. 1998. Wind-induced interference effects on buildings-a review of the state-of-art 20, 617-630.

Kondo, K., Murakami, S., Mochida, A. 1997. Generation of velocity fluctuations for inflow boundary condition of LES. Journal of Wind Engineering and Industrial Aerodynamics 67-68, 51-64.

Lam, K. M. and To, A. P. 2006. Reliability of numerical computation of pedestrian-level wind environment around a row of tall buildings Vol. 9.

Lam, K.M., H. Leung, M.Y., Zhao, J.G. 2008. Interference effects on wind loading of a row of closely spaced tall buildings. Journal of Wind Engineering and Industrial Aerodynamics 96, 562-583.

Lim, H.C., Thomas, T.G., Castro, I.P. 2009. Flow around a cube in a turbulent boundary layer: LES and experiment. Journal of Wind Engineering and Industrial Aerodynamics 97, 96-109.

Lund, T.S. 1998. Generation of turbulent inflow data for spatially-developing boundary layer simulations, 233-258.

Mochida, A., Tominaga, Y., Murakami, S., Yoshie, R., Ishihara , O., R. 2002. Comparison of various k–ε models and DSM applied to flow around a high-rise building—Report on AIJ cooperative project for CFD prediction of wind environment Vol. 5 No. 2~4, 227-244.

Murakami, S. 1998. Overview of turbulence models applied in CWE–1997. Journal of Wind Engineering and Industrial Aerodynamics 74-76, 1-24.

Nozawa, K., Tamura, T. 2002. Large eddy simulation of the flow around a low-rise building immersed in a rough-wall turbulent boundary layer. Journal of Wind Engineering and Industrial Aerodynamics 90, 1151-1162.

Paterson, D.A. 1993. Predicting r.m.s. pressures from computed velocities and mean pressures. Journal of Wind Engineering and Industrial Aerodynamics 46-47, 431-437.

Princevac, M., Baik, J., Li, X., Pan, H., Park, S. Lateral channeling within rectangular arrays of cubical obstacles. Journal of Wind Engineering and Industrial Aerodynamics In Press, Corrected Proof.

Senthooran, S., Lee, D., Parameswaran, S. 2004. A computational model to calculate the flow-induced pressure fluctuations on buildings. Journal of Wind Engineering and Industrial Aerodynamics 92, 1131-1145.

Stathopoulos, T., Wu, H. 2004. Computational Fluid Dynamics (CFD) for pedestrian winds. Proceedings of the 2004 Structures Congress, Nashville, TN.

Tamura, T., Nozawa, K., Kondo, K. 2008. AIJ guide for numerical prediction of wind loads on buildings. Journal of Wind Engineering and Industrial Aerodynamics 96, 1974-1984.

Thepmongkorn, S., Wood, G.S., Kwok, K.C.S. 2002. Interference effects on wind-induced coupled motion of a tall building. Journal of Wind Engineering and Industrial Aerodynamics 90, 1807-1815.

Tominaga, Y., Mochida, A., Murakami, S., Sawaki, S. 2008a. Comparison of various revised k–ε models and LES applied to flow around a high-rise building model with 1:1:2 shape placed within the surface boundary layer. Journal of Wind Engineering and Industrial Aerodynamics 96, 389-411.

Tominaga, Y., Mochida, A., Yoshie, R., Kataoka, H., Nozu, T., Yoshikawa, M., Shirasawa, T. 2008b. AIJ guidelines for practical applications of CFD to pedestrian wind environment around buildings. Journal of Wind Engineering and Industrial Aerodynamics 96, 1749-1761.

Werner, H., H. Wengle, H. 1991. Large-eddy simulation of turbulent flow over and around a cube in a plate channel. Proceeding of the 8th Symposium on Turbulent Shear Flows 19(4),155-165.

Wright, N.G., Easom, G.J. 2003. Non-linear k–e turbulence model results for flow over a building at full-scale. Applied Mathematical Modeling 27(12), 1013-1033.

Yoshie, R., Mochida, A., Tominaga, Y., Kataoka, H., Harimoto, K., Nozu, T., Shirasawa, T. 2007. Cooperative project for CFD prediction of pedestrian wind environment in the Architectural Institute of Japan. Journal of Wind Engineering and Industrial Aerodynamics 95, 1551-1578.

Zhang, A., Gu, M. 2008. Wind tunnel tests and numerical simulations of wind pressures on buildings in staggered arrangement. Journal of Wind Engineering and Industrial Aerodynamics 96, 2067-2079.